

# Hole concentration dependence of the magnetic moment in superconducting and insulating $\text{La}_{2-x}\text{Sr}_x\text{CuO}_4$

S. Wakimoto\* and R. J. Birgeneau†

Department of Physics and Center for Materials Science and Engineering, Massachusetts Institute of Technology, Cambridge, Massachusetts 02139

Y. S. Lee

National Institute of Standards and Technology, NCNR, Gaithersburg, Maryland 20889

G. Shirane

Physics Department, Brookhaven National Laboratory, Upton, New York 11973

(December 2, 2024)

Recent neutron scattering measurements on the  $\text{La}_{2-x}\text{Sr}_x\text{CuO}_4$  system have revealed a drastic change of the incommensurate static spin correlations from diagonal in the insulating region to parallel in the superconducting region. We report the doping dependence of the ordered magnetic moment for the hole concentration region  $0.03 \leq x \leq 0.12$ , focusing on the relationship between the static magnetism and the superconductivity. The elastic magnetic crosssection decreases monotonically with increasing  $x$  for  $0.03 \leq x \leq 0.07$ . We find that the ordered magnetic moment  $\mu$  varies from  $\sim 0.18$  ( $x = 0.03$ ) to  $\sim 0.06 \mu_B/\text{Cu}$  ( $x = 0.07$ ). No significant anomaly is observed at the insulator-superconductor boundary ( $x \sim 0.055$ ). The elastic magnetic crosssection is enhanced in the vicinity of  $x = 0.12$  whose resolution limited width peaks are observed in neutron scattering measurements and where the apparent magntic and superconducting transitions coincide.

## I. INTRODUCTION

The high- $T_C$  superconducting material  $\text{La}_{2-x}\text{Sr}_x\text{CuO}_4$  exhibits a remarkable dependence of both its magnetism and its conductivity on the hole concentration  $x$ . (Ref.1) In particular, the discovery of dynamic *incommensurate* (IC) spin correlations in superconducting samples<sup>2-4</sup> stimulated investigations of the correlation between the microscopic magnetism and the high- $T_C$  superconductivity. Specifically, in superconducting samples inelastic IC magnetic peaks have been observed by neutron-scattering experiments at the IC positions with  $\alpha \sim 45^\circ$  in polar coordinates as shown in the right inset of Fig.1(a). We refer to these type of satellite peaks as “parallel” incommensurate (PIC) peaks. Systematic neutron scattering experiments in the superconducting region by Yamada *et al.*<sup>5</sup> revealed that the incommensurability  $\delta$  of the PIC peaks<sup>6</sup> follows the linear relation  $\delta = x$  for  $0.06 \leq x \leq 0.12$ . Very sharp *elastic* IC magnetic peaks are also reported<sup>7,8</sup> at the same PIC positions only in the vicinity of the special  $1/8$  hole concentration.

On the other hand, Wakimoto *et al.*<sup>9,10</sup> found a new class of *elastic* IC magnetic peaks in the insulating  $x = 0.04$  and  $0.05$  samples at the positions with  $\alpha \sim 90^\circ$  as shown in the left inset of Fig.1(a). We refer to these peaks as “diagonal” incommensurate (DIC) peaks. Matsuda *et al.*<sup>11</sup> confirmed the existence of the static DIC phase down to Sr concentrations as low as  $x = 0.024$  as well as the linear relation  $\delta = x$  in the insulating DIC phase.<sup>12</sup> The detailed nature of the transition from the insulator

to the superconductor and concomitantly the DIC to the PIC magnetic phase has been also clarified recently.<sup>13</sup>

It is clear from the phenomenological evidence discussed above that the IC nature of both the “static” and “dynamic” magnetic correlations relates closely to the superconductivity. However, it is not yet fully understood what the intrinsic relation is between the *static* moment and the superconductivity. Some previous neutron scattering studies have reported an enhancement of the static component at the  $1/8$  hole concentration<sup>7,8,14</sup> while other experimental techniques<sup>15</sup> have suggested a competitive relation. On the other hand, coexistence of the superconductivity and static IC magnetic order has been reported in the stage-4  $\text{La}_2\text{CuO}_{4+\delta}$  by Lee *et al.*<sup>16</sup> Furthermore, systematic  $\mu\text{SR}$ <sup>17</sup> and NMR<sup>18</sup> measurements from the insulating region to the underdoped superconducting region have revealed that static (or quasi-static) magnetic order exists up to  $x = 0.10$  and that the spin glass ordering temperature varies continuously across the insulator-superconductor boundary  $x \sim 0.055$ . These results suggest that superconductivity and static magnetic order are at least compatible.

To understand the intrinsic relation between the superconductivity and the static magnetic order we have carried out a quantitative comparison of the elastic magnetic neutron-scattering crosssection over the concentration range  $0.03 \leq x \leq 0.12$  taking into account the IC peak geometry. We deduce the ordered magnetic moment which contributes to the elastic cross-section, and find that the ratio between the statically ordered and

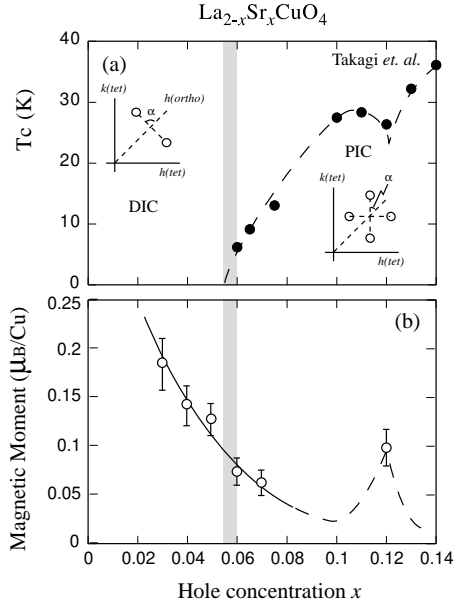


Figure 1

FIG. 1.  $x$ -dependence of (a) superconducting transition temperature  $T_c$  referred from Ref.25 and (b) magnetic moment. The insets show the IC peak geometries in the reciprocal space. Moment value for  $x = 0.12$  is reported in Ref.24. Solid and dashed lines are guides to the eye.

dynamically fluctuating components changes systematically with  $x$ . The  $\text{Cu}^{2+}$  moment in the undoped  $\text{La}_2\text{CuO}_4$  is known to be  $\sim 0.6 \mu_B/\text{Cu}$ . Throughout this paper, we use Miller indices based on the orthorhombic *Bmab* structure.

## II. EVALUATION OF MAGNETIC MOMENT FOR $X = 0.05$

### A. Fundamental formula

Before we discuss the  $x$ -dependence of the magnetic moment, we first present in this section the evaluation procedure for the magnetic moment in  $\text{La}_{1.95}\text{Sr}_{0.05}\text{CuO}_4$ . Once the moment in  $x = 0.05$  has been determined, the moments in the  $x = 0.03$  and 0.04 samples can be estimated from the relative integrated intensity of the magnetic IC peaks as discussed in the next section.

From the definition of the magnetic structure factor, the calculated integrated intensity of the magnetic peaks can be described using the magnetic moment  $\mu$  as below.

$$|F_M|_{cal}^2 = p^2 f^2(\mathbf{Q}) \cdot n^2 \cdot \mu^2 \cdot \sin^2 \beta \cdot |F(h, k, l)|^2. \quad (1)$$

In this formula,  $p f(\mathbf{Q})$  is the neutron magnetic scattering length, where  $p = 0.2696 \text{ cm}$  for  $S = 1/2$  spins.  $f(\mathbf{Q})$  is the  $\mathbf{Q}$ -dependent magnetic form factor for the  $\text{Cu}^{2+}$  spin which has been previously measured.<sup>19</sup> The parameters  $n$ ,  $\beta$  and  $F(h, k, l)$  represent the number of spins in a magnetic unit cell, the angle of the  $\text{Cu}^{2+}$  spins with

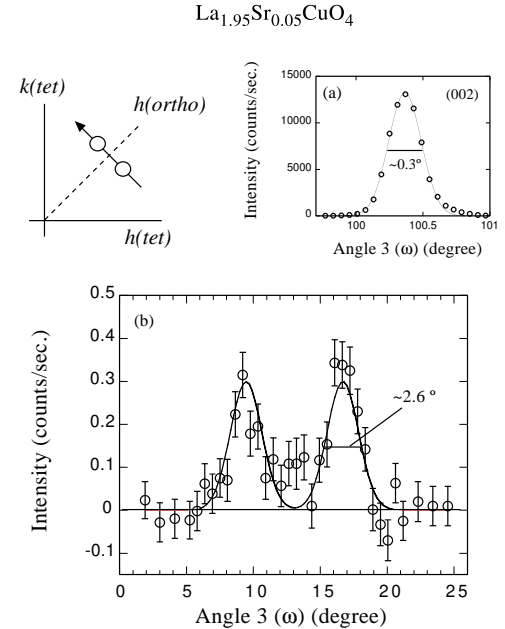


FIG. 2. Peak profiles of (a) the (002) peak and (b) the IC elastic magnetic peaks for  $x = 0.05$ . Both are measured by changing sample rotation angle  $\omega$ . The scan profile for (b) is shown in the left upper panel. Solid lines are fits by the Gaussian function.

respect to the scattering vector, and the magnetic structure factor, respectively. The spin structure in the  $x = 0.05$  sample at low temperatures can be understood by a spin glass cluster model<sup>10</sup> in which each cluster has the undoped  $\text{La}_2\text{CuO}_4$  type spin structure with random spin orientation in the plane. With this structure,  $n = 4$  and  $F(h, k, l) = 1 + e^{-\pi i(k+l)} - e^{-\pi i(h+k)} - e^{-\pi i(l+h)}$ . Since the spin direction in each cluster is random, the factor  $\sin^2 \beta$  in Eq. 1 should be modified to be  $\langle \sin^2 \beta \rangle = 1/2$ , where  $\langle \rangle$  means an average over all of the clusters.

The relation between the calculated and observed integrated intensities is

$$\frac{|F_M|_{cal}^2}{|F_N|_{cal}^2} = \frac{|F_M|_{obs}^2}{B \cdot |F_N|_{obs}^2} = A, \quad (2)$$

where  $B$  is the extinction factor for the nuclear Bragg peak and the ratio  $A$  is a constant which can be determined experimentally. The indices  $M$  and  $N$  mean magnetic and nuclear scattering, respectively. From Eqs. 1 and 2, the magnetic moment  $\mu$  can be described as

$$\mu^2 = \frac{A \cdot |F_N|_{cal}^2}{p^2 \cdot f^2(\mathbf{Q}) \cdot n^2 \cdot \langle \sin^2 \beta \rangle \cdot |F(h, k, l)|^2}. \quad (3)$$

### B. Integrated intensity

In order to determine the parameter  $A$ , we made scans across the IC magnetic peaks and the (002) nuclear Bragg

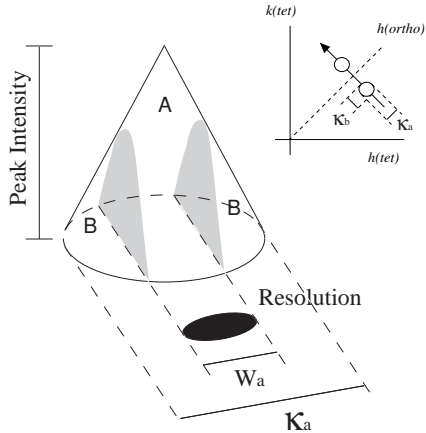


FIG. 3. Schematic figure showing the broad peak and instrumental resolution.  $\kappa_a$  and  $\kappa_b$  correspond to the full width at the half maximum of the IC magnetic peak along the orthorhombic  $a^*$  and  $b^*$  axis.  $W_a$  is the instrumental resolution width along the  $a^*$  axis.

peak without changing the spectrometer configuration using the same  $x = 0.05$  crystal studied in Ref.8. The measurements were performed on the BT9 thermal neutron triple-axis spectrometer installed at the NIST research reactor with the collimation sequence 20'-20'-S-20'-open and an incident neutron energy of 14.6 meV. A PG filter was installed to eliminate contamination from higher-order neutrons. For the evaluation of  $|F_N|_{obs}^2$  and  $|F_N|_{cal}^2$ , we utilized the (002) peak which was found to have a small extinction factor ( $B \sim 1$ ) in a preliminary crystallographic experiment. Actual scan profiles of the (002) peak and the IC peaks are shown in Fig.2(a) and (b), respectively. The scan trajectory for Fig.2(b) is shown in the upper panel. Both scans were made by changing only the sample rotation angle  $\omega$ .

Usually, integrated intensities for “resolution limited” peaks, such as nuclear Bragg peaks, can be directly obtained from  $\omega$ -scans with  $|F_N|_{obs}^2 = R \int I(\omega) d\omega$ . Here  $R$  is the Lorentz factor  $1/\sin(2\theta)$  where  $2\theta$  is the scattering angle, and  $I(\omega)$  is the measured intensity. However, the IC magnetic peaks in  $x = 0.05$  have widths which are larger than the resolution. This is schematically illustrated in Fig.3. If the peak width  $\kappa_a$  is larger than the resolution width  $W_a$ , the integration along the one dimensional trajectory shown by an arrow gives integrated intensity only of the A part of the peak cone, and the intensities in the B parts will be missed.

In our measurements of the IC peaks around (100), the  $\kappa_a$  and  $W_a$  values are 0.094 and  $0.0165 \text{ \AA}^{-1}$ , respectively, and  $\kappa_b$  is  $0.045 \text{ \AA}^{-1}$ . In this configuration, the actual in-plane integrated intensity for one IC peak should be described as  $|F'|_{obs}^2 = 1.6R \int I(\omega) d\omega$ . The factor 1.6 is the volume ratio of the total peak cone and the A part in Fig.3.

The same consideration must be taken into account for the peak width along the direction perpendicular to the scattering plane, that is, the  $c^*$  direction. As reported in Ref.10, the  $L$ -dependence of the IC peak in the  $x =$

0.05 sample is very broad. Thence, we should utilize the intensity integrated over the Brillouin zone, that is, for  $-1 \leq L \leq 1$ . From the vertical instrumental resolution ( $\sim 0.13 \text{ \AA}^{-1}$ ), the correction factor for the peak spread along the  $c^*$  direction is estimated to be  $4(\pm 0.5)$  which multiplies  $|F'|_{obs}^2$ .

To evaluate the parameter  $A$ , we utilized  $|F_M|_{obs}^2 = \sum |F'|_{obs}^2$ , where the summation is made for every IC peaks around the (100) position for all orthorhombic twin domains. With the procedure above and Eq. 3, we finally obtained  $\mu \sim 0.13(\pm 0.02) \mu_B/\text{Cu}$  for  $x = 0.05$ .

### III. RESULTS AND DISCUSSION

The magnetic properties of the  $x = 0.03$  and  $0.04$  samples are essentially the same as those of the  $x = 0.05$  system showing spin glass behavior<sup>21</sup> and the DIC peaks.<sup>10,11</sup> These facts suggest the same magnetic structure in these compositions. Therefore, the magnetic moments for  $x = 0.03$  and  $0.04$  can be estimated by a direct comparison of  $|F_M|_{obs}^2$  normalized by sample volume. For  $x = 0.06$  and  $0.07$ , we also compared the normalized  $|F_M|_{obs}^2$  from the elastic crosssections reported in Ref.11 which demonstrated that the  $x = 0.06$  sample shows DIC and PIC components while the  $x = 0.07$  sample shows only PIC component. The magnetic moments for these compositions are also evaluated from their normalized  $|F_M|_{obs}^2$  calculated by summation of the integrated intensities of all the IC peaks around (100).

We note that the  $L$ -dependence of the IC peaks in the  $x = 0.024$  material as reported by Matsuda *et al.*<sup>11</sup> is clearer than that in the  $x = 0.05$  sample. This means that the correction factor for the peak spread along the  $c^*$  direction should decrease with decreasing  $x$ . Thence, we estimated the correction factors for  $x = 0.03$  and  $0.04$  to be between 3 and 4, while the lower value 3 was calculated from the  $L$ -dependence of  $x = 0.024$ . The ambiguity of this factor is shown as error bars in Fig.1(b). For  $x = 0.06$  and  $0.07$ , the  $L$ -correction factor of  $4(\pm 0.5)$  was utilized.

The resultant magnetic moments together with that for  $x = 0.12$  reported by Kimura *et al.*<sup>22</sup> are summarized in Fig.1(b). Figure 1(a) shows the  $x$ -dependence of  $T_C$  reported by Takagi *et al.*<sup>23</sup> First we discuss the  $x$ -dependence of the magnetic moment near the insulator-superconductor boundary  $x \sim 0.055$ . The magnetic moment decreases monotonically across the boundary although we cannot exclude the possibility of a small drop at the boundary. In a previous study in the lightly doped region, it was reported that the elastic magnetic cross-section was constant for  $0.03 \leq x \leq 0.05$  and suddenly decreased at the insulator-superconductor boundary.<sup>20</sup> However, in that analysis, the integration of the cross-section was made only along the one-dimensional scan so that the crosssection outside the instrumental resolution was not properly taken into account. Moreover, the correct IC peak geometry was not known at that time.

Other characteristics of the elastic IC peak have been reported<sup>13</sup> to be continuous across the insulator-superconductor boundary, such as the peak width and the onset temperatures where the elastic IC peaks become observable. Thus, the only dramatic change in the magnetic state at the boundary is the change of the IC modulation direction. This collection of evidence suggests that it is the transition from the DIC to PIC magnetic state rather than any decrease of the static ordered component which strongly correlates with superconductivity.

In Fig.1(b) we draw the dashed line as a guide so that the moment has a sharp maximum at  $x = 0.12$  since the sharp and intense IC elastic peaks have only been observed in the vicinity of  $x = 0.12$ .<sup>8</sup> It should be noted that the ordered phases in samples with  $0.03 \leq x \leq 0.07$  compared with that in  $x = 0.12$  are different. The former has small correlation length  $\xi \sim 20 \text{ \AA}$ , while the latter shows resolution-limited peaks which correspond to  $\xi \geq 200 \text{ \AA}$ . Such a long range ordered state might affect the superconductivity differently from the quasi-static glassy state observed in  $0.03 \leq x \leq 0.07$ . Further study of the intrinsic difference between these ordered state is required to clarify the relation between the static magnetic order and the superconductivity.

Finally, we briefly mention the recent results of  $\mu$ SR measurements on the LSCO system by Uemura *et al.*<sup>24</sup> They reported that the ordered magnetic moment is almost constant at  $\sim 0.3 \mu_B/\text{Cu}$  in  $\text{La}_{1.88}\text{Sr}_{0.12}\text{CuO}_4$  and stage-4  $\text{La}_2\text{CuO}_{4+\delta}$ , however they infer that the volume fraction which contributes the statically ordered signal may be different. We should note that the systematic change of the ordered moment in the lightly doped region as reported in this paper may be caused by the same feature, that is, it is possible that only the volume fraction of the ordered phase instead of the ordered moment varies with  $x$ , since we cannot uniquely determine the volume fraction from our neutron scattering measurements.

#### IV. ACKNOWLEDGMENTS

We thank Y. Endoh, M. Fujita, K. Hirota, H. Hiraka, M. A. Kastner, H. Kimura, S. H. Lee, M. Matsuda, T. Uemura, K. Yamada and A. Zeludev for valuable discussions. The present work was supported by the US-Japan Cooperative Research Program on Neutron Scattering. The work at MIT was supported by the NSF under Grant No. DMR001 and by the MRSEC Program of the National Science Foundation under Award No. DMR98-08941. The work at Brookhaven National Laboratory was carried out under Contract No. DE-AC02-98CH10886, Division of Material Science, U. S. Department of Energy. The work at NIST is based upon activities supported by the National Science Foundation under Agreement No. DMR-9423101.

\* Also at Brookhaven National Laboratory, Upton, New York 11973

† Present address: University of Toronto, Toronto, Ontario, Canada M5S 1A7

---

<sup>1</sup> M. A. Kastner, R. J. Birgeneau, G. Shirane and Y. Endoh, Rev. Mod. Phys., **70**, 897 (1998).

<sup>2</sup> H. Yoshizawa, S. Mitsuda, H. Kitazawa and K. Katsumata, J. Phys. Soc. Jpn. **57**, 3686 (1988);

<sup>3</sup> R. J. Birgeneau, Y. Endoh, Y. Hidaka, K. Kakurai, M. A. Kastner, T. Murakami, G. Shirane, T. R. Thurston and K. Yamada, Phys. Rev. B **39**, 2868 (1989); T. R. Thurston, R. J. Birgeneau, M. A. Kastner, N. W. Preyer, G. Shirane, Y. Fujii, K. Yamada, Y. Endoh, K. Kakurai, M. Matsuda, Y. Hidaka and T. Murakami, Phys. Rev. B **40**, 4585 (1989).

<sup>4</sup> S. -W. Cheong, G. Aeppli, T. E. Mason, H. A. Mook, S. M. Hayden, P. C. Canfield, Z. Fisk, K. N. Klausen and J. L. Martinez, Phys. Rev. Lett. **67**, 1791 (1991).

<sup>5</sup> K. Yamada, C. H. Lee, K. Kurahashi, J. Wada, S. Wakimoto, S. Ueki, H. Kimura, Y. Endoh, S. Hosoya, G. Shirane, R. J. Birgeneau, M. Greven, M. A. Kastner and Y. J. Kim, Phys. Rev. B **57**, 6165 (1998).

<sup>6</sup>  $\delta$  can be defined by the distance between  $(\pi, \pi)$  and the PIC peak positions  $(1/2 \pm \delta, 1/2)$  and  $(1/2, 1/2 \pm \delta)$  in the tetragonal  $I4/mmm$  notation.

<sup>7</sup> T. Suzuki, T. Goto, K. Chiba, T. Shinoda, T. Fukase, H. Kimura, K. Yamada, M. Ohashi and Y. Yamaguchi, Phys. Rev. B **57**, 3229 (1998).

<sup>8</sup> H. Kimura, K. Hirota, H. Matsushita, K. Yamada, Y. Endoh, S. -H. Lee, C. F. Majkrzak, R. Erwin, G. Shirane, M. Greven, Y. S. Lee, M. A. Kastner, and R. J. Birgeneau, Phys. Rev. B **59**, 6517 (1999) and private communication.

<sup>9</sup> S. Wakimoto, G. Shirane, Y. Endoh, K. Hirota, S. Ueki, K. Yamada, R. J. Birgeneau, M. A. Kastner, Y. S. Lee, P. M. Gehring and S. H. Lee, Phys. Rev. B **60**, R769 (1999).

<sup>10</sup> S. Wakimoto, R. J. Birgeneau, M. A. Kastner, Y. S. Lee, R. Erwin, P. M. Gehring, S. H. Lee, M. Fujita, K. Yamada, Y. Endoh, K. Hirota and G. Shirane, Phys. Rev. B **61**, 3699 (2000).

<sup>11</sup> M. Matsuda, M. Fujita, K. Yamada, R. J. Birgeneau, M. A. Kastner, H. Hiraka, Y. Endoh, S. Wakimoto and G. Shirane, cond-mat0003466. (Phys. Rev. B. accepted.)

<sup>12</sup>  $\delta$  of DIC peaks is defined by a distance between  $(\pi, \pi)$  and DIC peaks in the *tetragonal* reciprocal lattice unit. Therefore, DIC peak positions can be described as  $(1, \pm\sqrt{2}\delta)$  in the orthorhombic *Bmab* notation.

<sup>13</sup> M. Fujita, K. Yamada, H. Hiraka, S. H. Lee, P. M. Gehring, S. Wakimoto, G. Shirane, unpublished.

<sup>14</sup> J. M. Tranquada, B. J. Sternlieb, J. D. Axe, Y. Nakamura, S. Uchida, Nature **375**, 561 (1995); J. M. Tranquada, J. D. Axe, N. Ichikawa, Y. Nakamura, S. Uchida and B. Nachumi, Phys. Rev. B **54**, 7489 (1996).

<sup>15</sup> For example, by muon spin rotation ( $\mu$ SR) measurement in K. Kumagai, K. Kawano, I. Watanabe, K. Nishiyama, and K. Nagamine, J. Supercond. **7**, 63 (1994). By nuclear

magnetic resonance (NMR) measurement in T. Goto, S. Kazama, K. Miyagawa, and T. Fukase, *J. Phys. Soc. Jpn.* **63**, 3494 (1994).

<sup>16</sup> Y. S. Lee, R. J. Birgeneau, M. A. Kastner, Y. Endoh, S. Wakimoto, K. Yamada, R. W. Erwin, S. H. Lee and G. Shirane, *Phys. Rev. B* **60**, 3643 (1999).

<sup>17</sup> Ch. Niedermayer, C. Bernhard, T. Blasius, A. Golnik, A. Moodenbaugh, and J. I. Budnick, *Phys. Rev. Lett.* **80**, 3843 (1998).

<sup>18</sup> F. C. Chou, F. Borsa, J. H. Cho, D. C. Johnston, A. Lascialfari, D. R. Torgeson and J. Ziolo, *Phys. Rev. Lett.* **71**, 2323 (1993).

<sup>19</sup> S. Shamoto, M. Sato, J. M. Tranquada, B. J. Sternlieb and G. Shirane, *Phys. Rev. B* **48**, 13817 (1993).

<sup>20</sup> S. Wakimoto, K. Yamada, S. Ueki, G. Shirane, Y. S. Lee, S. H. Lee, M. A. Kastner, K. Hirota, P. M. Gehring, Y. Endoh and R. J. Birgeneau, *J. Phys. Chem. Solids* **60**, 1079 (1999).

<sup>21</sup> S. Wakimoto, S. Ueki, Y. Endoh and K. Yamada, *Phys. Rev. B* **62**, 3547 (2000).

<sup>22</sup> H. Kimura, H. Matsushita, K. Hirota, Y. Endoh, K. Yamada, G. Shirane, Y. S. Lee, M. A. Kastner, R. J. Birgeneau, *Phys. Rev. B* **61**, 14366 (2000) and private communication.

<sup>23</sup> H. Takagi, T. Ido, S. Ishibashi, M. Uota, and S. Uchida, *Phys. Rev. B* **40**, 2254 (1989).

<sup>24</sup> T. Uemura, private communication; T. Uemura, Y. S. Lee and R. J. Birgeneau, unpublished.